Desalination and Water Treatment
www.deswater.com
5 (2009) 91–98
1944-3994/1944-3986

Comparing the desalination performance of SMM blended polyethersulfone to SMM blended polyetherimide membranes by direct contact membrane distillation

M. Qtaishat[a]*, T. Matsuura[b], M. Khayet[c], K.C. Khulbe[b]

[a]*Chemical Engineering Department, University of Jordan, Amman 19942, Jordan*
Tel: +962 6 535 5000, ext. 22902; Fax: +962 6 535 5588; email: mrasool78@yahoo.com
[b]*Industrial Membrane Research Laboratory, Department of Chemical Engineering, University of Ottawa, 161 Louis Pasteur, PO Box 450, Stn. A, Ottawa, Ontario K1N 6N5, Canada*
[c]*Faculty of Physics I, University Complutense of Madrid, Av. Complutense s/n, 28040, Madrid, Spain*

Received 31 August 2008; Accepted 12 April 2009

ABSTRACT

This study aims to compare the effect of host hydrophilic polymer on novel hydrophobic/hydrophilic composite membrane characteristics and desalination performance by direct contact membrane distillation (DCMD). Two different polymers are used for the host polymer: polyethersulfone (PES) and polyetherimide (PEI). The membranes were prepared by the phase inversion method by blending surface modifying macromolecules (SMM) into the host hydrophilic polymer (PES and PEI). The membranes were characterized using a wide variety of characterization techniques including the gas permeation test, measurement of the liquid entry pressure of water (*LEPw*), scanning electronic microscopy (SEM), atomic force microscopy (AFM) and contact angle measurement. Furthermore, the membranes were tested by DCMD for desalination of 0.5 M NaCl solution and the results were compared to commercial polytetrafluoroethylene (PTFE) membranes (FGLP 1425, Millipore). The effects of the type of host polymer on membrane morphology and characteristics were identified, which enabled us to link membrane morphology to membrane performance. The PES membrane yielded superior flux to that of the commercial membrane and the PEI membrane when their performance was compared. This result could be attributed to the fact that the nSMM/PES had a higher pore size/porosity ratio and lower *LEPw* than the nSMM/PEI membrane. It is worth mentioning that all prepared membranes were tested successfully for the desalination application. In other words, NaCl concentrations in the permeate were below 200 ppm.

Keywords: Direct contact membrane distillation; Desalination; Hydrophobic/-philic composite membranes; Surface modifying macromolecules; Polyetherimide, Polyethersulfone

1. Introduction

Membrane distillation (MD) is a non-isothermal separation process in which a microporous hydrophobic membrane acts as a physical barrier separating a hot feed solution from a cooling chamber containing either a liquid or a gas. In the direct contact membrane distillation (DCMD) configuration, a cold liquid solution is allowed to flow through the permeate side of the membrane in order to condense the vapor that has migrated through the membrane pores from the hot feed solution [1–7].

*Corresponding author.

Presented at EuroMed 2008, Desalination for Clean Water and Energy Cooperation among Mediterranean Countries of Europe and the MENA Region, 9–13 November 2008, King Hussein Bin Talal Convention Center, Dead Sea, Jordan.

Despite all of the reported MD advantages [1], the process has not been commercialized yet for large-scale desalination plants. The reason is the relatively lower MD flux compared to the production of the well established commercialized desalination processes such as reverse osmosis. This is stemming from the lack of a rational membrane design procedure to satisfy the requirements for successful MD membranes, which are, mainly, low conductive heat flux (i.e. low heat loss by conduction through the membrane matrix) and high mass transfer flux.

Commercial hydrophobic membranes made of polypropylene (PP), poly(vinylidene fluoride) (PVDF) or polytetrafluoroethylene (PTFE) have so far been used in MD experiments although these membranes were marketed for microfiltration and ultrafiltration processes. Recently, however, more attention has been paid to the preparation of membranes specifically designed for MD applications. Most of these attempts were previously summarized [6].

One of the most promising attempts is the composite hydrophobic/hydrophilic membranes. Khayet et al. [8–10] were the initiator of the hydrophobic/hydrophilic composite membrane concept in MD where hydrophobic surface modifying macromolecules (SMM41) were synthesized and blended with the host hydrophilic polymer (PEI). At a later stage; Suk et al. [11] developed a new surface modifying macromolecule (nSMM) and prepared SMM blended composite membranes for MD using polyethersulfone (PES) as the host hydrophilic polymer. It was shown that this type of membranes satisfies all the requirements for achieving high flux MD membranes [8,11].

The hydrophobic/hydrophilic composite membrane is prepared by the phase inversion method in a single casting step. During the casting step, the SMMs migrates to the air/polymer interface since they have lower surface energy [8]. Earlier studies [8–11] focused on the effect of the SMM type used to fabricate hydrophobic/hydrophilic membranes. On the other hand, the effect of membrane casting solution composition on the membrane performance and characteristics has not been studied coherently.

In this study, the nSMM was used to prepare the SMM blended PES and PEI composite membranes. The membranes were prepared by a single casting step via the phase inversion method as described in an earlier study [8]. The membranes were characterized using a wide variety of characterization techniques including the gas permeation test, measurement of the liquid entry pressure of water (*LEPw*), scanning electronic microscopy (SEM), atomic force microscopy (AFM) and contact angle measurement (CA).

The main objective of this work is to study the effect of the hydrophilic polymer type on membrane characteristics as well as its DCMD performance when distilled water or 0.5 M NaCl solution was used as a feed. The results were compared to those of the commercial PTFE membrane (FGLP 1425, Millipore, USA). The prepared membranes seem promising for practical application in desalination by DCMD. An objective to link the characteristics of the composite hydrophobic/hydrophilic composite membrane to DCMD performance seems achieved in this study. This improves the overall understanding of the principle of the hydrophobic/hydrophilic composite membrane in MD, which will open wide venues toward developing membranes specifically for MD applications.

2. Experimental

2.1. Materials

All chemicals used in this work and their chemical abstract service (CAS) number are enlisted in Table 1. The average molecular weight (M_w) of the PEI and the PES used in this study are 15 and 30.8 kDa, respectively. The

Table 1
Materials used in this work.

Material description	CAS no.	Source
4,4-Methylene bis(phenyl isocyanate) (MDI, 98%)	101-68-8	Sigma-Aldrich, St. Louis, MO, USA
α,ω-Aminopropyl poly(dimethyl siloxane) (PDMS) of average molecular weight 900	106214-84-0	Shin-Etsu Chemical Tokyo, Japan
Zonyl fluorotelomer intermediate, 2-(Perfluoroalkyl)ethanol, (FAE, BA-L of average M_n 443 and 70 wt% fluorine	678-39-7	DuPont product, supplied by Aldrich Chemical Milwaukee, WI, USA
N,N-Dimethylacetamide (DMAc, anhydrous 99.8%)	127-19-5	Sigma-Aldrich, St. Louis, MO, USA
1-Methyl-2-pyrrolidinone (NMP, anhydrous 99.5%)	112-14-1	Sigma-Aldrich, St. Louis, MO, USA
γ-Butyrolactone (GBL, 99+%)	96-48-0	Aldrich Chemical Milwaukee, WI, USA
Ethanol (anhydrous, 99+%)	64-17-5	Aldrich Chemical, Milwaukee, WI, USA
Tetrahydrofuran (THF, HPLC grade 99.9%)	109-99-9	Aldrich Chemical, Milwaukee, WI, USA
Polyetherimide (PEI, Ultem 1000, natural pallet) Specific gravity: 1.27	61128-46-9	General Electric Pittsfield, MA, USA
Polyethersulfone (PES, Radel A-300PNT)	25667-42-9	Amoco Polymer Alpharetta, GA, USA

commercial membrane used is PTFE (FGLP 1425), having a porosity of 0.70 and a nominal pore size of 0.25 μm supplied by Millipore (Billerica, MA, USA).

2.2. SMMs synthesis and characterization

The SMMs were synthesized using a two-step solution polymerization method [11]. The solvent *N,N*-dimethylacetamide (DMAc) was distilled at about 25°C under a pressure of 133.3 Pa. Methylene bis(*p*-phenyl isocyanate) (diphenylmethane diisocyanate, MDI) was also distilled at 150°C under 66.7 Pa (0.5 Torr). α,ω-aminopropyl poly(dimethyl siloxane) (PDMS) and 2-(perfluoroalkyl)ethanol (FAE) were degassed for 24 h under 66.7 Pa. The first polymerization step was conducted in a solution with a predetermined composition to form polyurea as a prepolymer from the reaction of MDI with PDMS. In the second step, the pre-polymer was end-capped by the addition of FAE, resulting in a solution of SMM. The composition of monomers for the synthesis of SMM is: MDI:PDMS:FAE = 3:2:2. The prepared SMM is named hereafter as nSMM2. The chemical structure of the prepared SMM is presented in Fig. 1.

The synthesized SMM was characterized for fluorine content, glass transition temperature and weight and number average molecular weights. *m*, *y*, and *q*, the repeating units shown in the chemical structure of the SMM (see Fig 1), were calculated from the average molecular weight of FAE, PDMS and SMM, respectively. Further details of SMM characterization are shown in a recent publication [12].

2.3. Membrane preparation

SMM modified PES and PEI membranes were prepared in a single casting step by the phase inversion method [8]. γ-butyrolactone (GBL) was used as a non-solvent additive for PEI and ethanol (ETOH) was used for PES. NMP was used as a solvent. A predetermined amount of PES or PEI was dissolved in a NMP/ETOH or NMP/GBL mixture. The polymer (PES or PEI) concentration in the casting solution was maintained at 12 wt%, while the amount of non solvent additive (ETOH or GBL) was maintained at 10 wt%. The added SMM concentration was 1.5 wt%. The resulted mixtures were stirred in an orbital shaker at room temperature for at least 48 h. Prior to their use, all the resulted polymer solutions were filtered through a 0.5 μm Teflon® filter and degassed at room temperature. The polymer solutions were cast on a smooth glass plate to a thickness of 0.30 mm using a casting rod at room temperature. The cast films together with the glass plates were immersed for 1 h in distilled water at room temperature. During gelation, it was observed that the membranes peeled off from the glass plate spontaneously. All the membranes were then dried at ambient conditions for 3 days. Two membranes were prepared, M1, which made of PES as the host polymer, and M2 based on PEI as the host polymer.

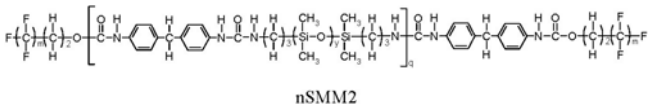

nSMM2

Fig. 1. Chemical structure of the prepared surface modifying macromolecules.

2.4. Membrane characterization

2.4.1. Measurement of the gas permeation test and liquid entry pressure of water

Measurement of liquid entry pressure of water (*LEPw*) and the gas permeation test were carried out for the prepared surface modified membranes. The gas permeation test was performed prior to the measurement of *LEPw*. The details of the system used together with the following method are explained in Khayet and Matsuura [13]. The product of average pore size and effective porosity per unit effective pore length ($r\varepsilon/L_p$) of the prepared membranes was determined by the gas permeation test. This ratio takes into account the tortuosity of the membrane pores.

In the present paper, the gas permeance through each dry membrane was measured at various transmembrane pressures, in the range of 10–100 kPa. In general, the gas permeance, *B*, for a porous medium contains both a diffusive term and a viscous term, the contribution of which depends on the applied pressure as reported by Carman [14]:

$$B=\frac{4}{3}\left(\frac{2}{\pi MRT}\right)^{0.5}\frac{r\varepsilon}{L_p}+\frac{P_m\ r^2\varepsilon}{8\mu RT\,L_p} \quad (1)$$

where *R* is the gas constant, *T* is the absolute temperature, *M* is the molecular weight of the gas, μ is the gas viscosity, P_m is the mean pressure within the membrane pore, *r* is the membrane pore radius, ε is the porosity, and L_p is the effective pore length.

Throughout all the gas permeation experiments, it was noticed that gas permeance was independent of P_m. Therefore, a diffusive mechanism seems to dominate the gas transport through the membrane pores, revealing the fact that the prepared membranes in this study have small pore sizes. Accordingly, the gas permeance is given, by ignoring the viscous term of Eq. (1), as [8]:

$$B=\frac{4}{3}\left(\frac{2}{\pi MRT}\right)^{0.5}\frac{r\varepsilon}{L_p} \quad (2)$$

This test was therefore useful in evaluating the ratio ($r\varepsilon/L_p$). Some of the gas permeation experiments were duplicated using different membrane sheets made from the same casting solution batch in order to evaluate the variance of the obtained values from sheet to sheet. Moreover, for each membrane, the measurement of the gas flow rate was made three times at a given gas pressure and the resulting values were averaged to obtain the membrane permeance value.

The measurements for the *LEPw* were then carried out as explained elsewhere [13]. The experiment was done three times using three different sheets made from the same casting solution batch. The results were averaged to obtain the final *LEPw* value of each membrane.

2.4.2. Scanning electron microscopy

The cross-section of the SMM blended PES/PEI membranes was analyzed by scanning electron microscopy SEM (JSM-6400 Jeol, Japan). The membranes were cut into pieces (3 mm wide and 10 mm long) and subsequently immersed in a liquid nitrogen reservoir for 5 s. While keeping the pieces in the liquid nitrogen, those were broken into two pieces by pulling from both ends. One of the broken pieces was mounted on a metal plate with carbon paste and gold-coated prior to use. The cross-section of the membranes at the broken parts was finally examined by SEM.

2.4.3. Atomic force microscopy observation

The morphology of the top surface (i.e. the hydrophobic surface) of the SMM/PES and SMM/PEI membranes was studied by atomic force microscopy (AFM). Details of the tapping mode (TM)-AFM technique are given elsewhere [15]. The membrane top surface is characterized in terms of roughness, pore size and size of nodule aggregates.

Pore sizes and nodule/nodular aggregate sizes were measured by visual inspection of line profiles from the obtained AFM images. To obtain the pore sizes and nodule/nodular aggregate sizes, cross-sectional line profiles were selected to traverse micron scan surface areas of the TM-AFM images. The diameters of nodules (i.e., light region or bright area, high peaks) or pores (i.e., dark area, low valleys, depression) were measured by a pair of cursors along the reference line. The horizontal distance between each pair of cursors was taken as the diameter of the nodule/nodular aggregate or pore.

The sizes of the pores or nodule/nodular aggregates are based on the average of at least 30 measurements. The roughness parameters obtained from AFM images should not be considered as the absolute roughness value. In the present study, the same tip was used for all experiments and all captured surfaces were treated in the same way. The evaluation of the roughness parameters of each membrane sample was based on various micron scan areas (i.e., 1×1 μm^2). The pore size distribution was calculated by the method described by Singh et al. [16].

2.4.4. Measurement of contact angle

The contact angle (CA) of both SMM/PES and SMM/PEI membranes was measured to study their hydrophobicity/-philicity. CA measurements were executed using the VCA-Optima (AST Products, MA, USA). Samples of 4 cm^2 area (2×2 cm) at random positions were prepared from each membrane. The samples were then placed on the glass sample plate and fixed with scotch tape. The equipment syringe filled with distilled water was installed to stand vertically. Two μl of water were deposited on the membrane surface. The CA was measured at five different spots on each membrane sample for both top and bottom surfaces.

2.5. DCMD experiments

The prepared SMM blended PES and PEI membranes were tested by the DCMD set-up shown in a previous study [8]. The central part of the system is a stainless steel cell composed of two cylindrical chambers. One of the chambers is connected to a heating system through its jacket to control the temperature of the liquid feed. The other chamber is connected to a cooling system to control the temperature of the permeate. The membrane is placed between the two chambers (feed side and permeate side). The hot feed solution is brought into contact with the hydrophobic top layer of the membrane and the cold permeate solution is in contact with the hydrophilic part of the membrane. The effective membrane area is 2.75×10^{-3} m^2. The bulk feed and permeate temperatures are measured, after steady state is reached, inside each chamber by a pair of sensors connected to a digital meter with an accuracy of ±0.1°C. Both the feed and permeate liquids are stirred inside the cell by graduated magnetic stirrers. The DCMD flux is calculated in every case by measuring the condensate collected in the permeate chamber for a predetermined period. The experiments are conducted first for pure water to determine the water vapour permeability of the membranes. Subsequently, aqueous solution of 0.5 M sodium chloride is used as feed.

The experiments are carried out under a temperature difference between the feed and permeate of 10°C. When distilled water was used as feed, the mean temperature was varied from 20 to 45°C, while the stirring rate was maintained at 500 rpm. When 0.5 M NaCl solution was used as feed, the mean temperature was 45°C and the stirring rate was 500 rpm. The concentration of both feed and permeate solutions is determined by a conductivity meter (712 ΩMetrohm). The solute separation factor, α, is

calculated using the following expression:

$$\alpha = \left(1 - \frac{C_p}{C_f}\right) * 100\% \quad (3)$$

where C_p and C_f are the NaCl concentration in the permeate and bulk feed solution, respectively.

3. Results and discussion

3.1. SMM and membrane characterization

The SMM characteristics, including the glass transition temperature (T_g), weight average molecular weight (M_w), number average molecular weight (M_n), fluorine content and the number of the structural repeating units are given in Table 2. The precise glass transition temperature (T_g) value could not be obtained for the SMM as the sample could be heated up to 280°C due to the limitation of higher temperature of the equipment. According to the SMMs chemical composition presented in Fig. 1, the value of m, the number of repeat unit of CF_2, was calculated from the FAE molecular weight. The value of y, the number of repeat unit of dimethylsiloxane, was calculated from the average molecular weight of PDMS. The value of q, the number of the urea repeat unit was calculated from the SMM weight average molecular weight.

The prepared SMM/PES and SMM/PEI membranes are called hereafter M1 and M2, respectively. The resulting CA data of those membranes are shown in Table 3. It was observed that the CA of the top side of the prepared membranes is higher than their bottom side. The CA of the top side was nearly equal to or higher than 90°, indicating that the top layer is sufficiently hydrophobic. In contrast, the CA of the bottom side of the membrane was lower than 90°, indicating the hydrophilicity of the bottom layer. This is evidence of the formation of composite hydrophobic/hydrophilic membranes by the phase inversion method in which hydrophobic nSMM is blended to a hydrophilic polymer.

Table 2
Surface modifying macromolecules (SMM) characteristics

Glass transition temperature, T_g (°C)	>280
Weight average molecular weight, M_w (10^4 g/mol)	2.71
Number average molecular weight, M_n (10^4 g/mol)	1.28
Fluorine content, F (wt%)	11.75
CF_2 repeating unit, m	7.58
Dimethylsiloxane repeating unit, y	9.81
Urea repeating unit, q	22.58

Table 3
Top and bottom contact angles of the prepared membranes

Membrane	CA (θ°)
M1	Top: 89.76 ± 3.34 Bottom: 62.69 ± 3.82
M2	Top: 91.93 ± 0.52 Bottom: 67.76 ± 3.29

The SEM images of the membranes cross-section are shown in Fig. 2. As can be seen, all the membranes are of asymmetric structure with a dense top-layer supported by a finger-like structure underneath. However, the bottom parts of the membranes are different. The finger-like structure of the membrane M1 (Fig. 2a) reaches the bottom side where small macro-voids were formed in the vertical direction. On the other hand, for the M2 membrane (Fig. 2b), the finger-like structure became more irregular in the middle of the cross-section and large macro-voids were formed in horizontal direction.

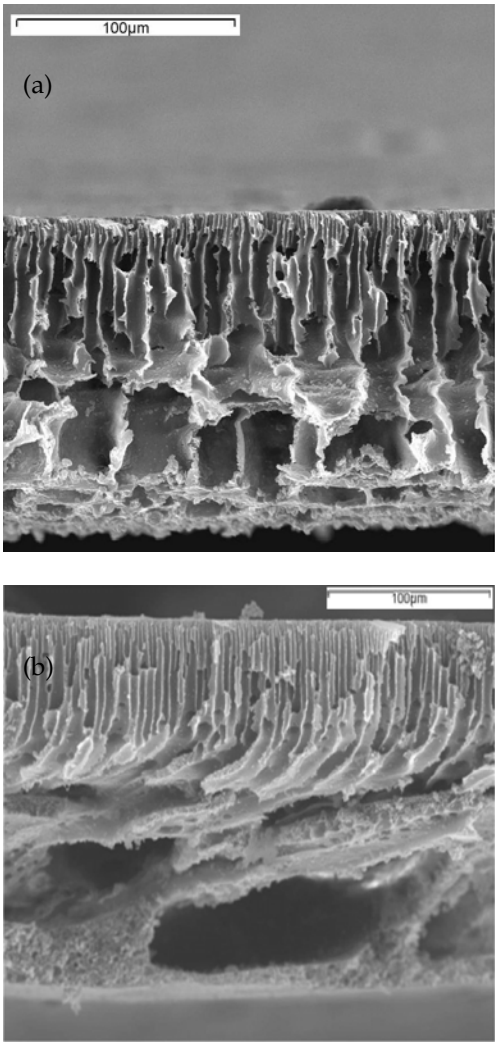

Fig. 2. SEM pictures of the cross-section of SMM/PES and SMM/PEI membranes: (a) M1; (b) M2.

AFM images of the SMM/PES (M1) and SMM/PEI (M2) top side membranes are shown in Fig. 3. The bright side is the highest point (nodule) and the dark region is the lowest point (pore). For analyzing the top surface characteristics, AFM image analysis program was used. Table 4 shows the top surface of the prepared membrane characteristics from the AFM analysis, including mean pore size, surface roughness and mean nodule size. As shown in Table 4, M1 membrane exhibited smaller mean pore size and larger nodule size compared to that of M2 membrane. From the mean pore size (d_p) and the geometric standard deviation (σ_p) data, pore size distribution of the laboratory-made membranes can be expressed by the probability density function [16]

The pore size distribution of M1 and M2 membranes are shown in Fig 4. As can be seen, M1 membrane exhibited narrower pore size distribution than the M2 membrane. The data for the *LEPw* and product of average pore size and effective porosity per unit effective pore length ($r\varepsilon/L_p$) are summarized in Table 5.

$$\frac{df(d_i)}{dd_i}=\frac{1}{d_i \ln\sigma_p\sqrt{2\pi}}\exp-\left[\frac{\left(\ln d_i-\ln d_p\right)^2}{2\left(\ln\sigma_p\right)^2}\right] \quad (4)$$

(a)

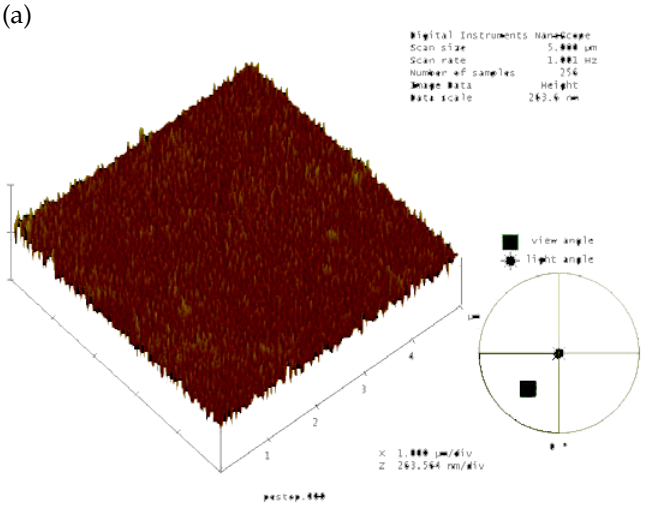

(b)

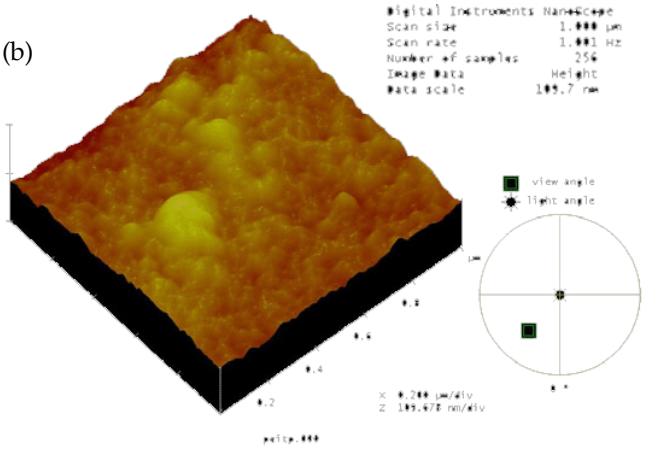

Fig. 3. AFM images of the top surface of SMM/PES and SMM/PEI membranes: (a) M1; (b) M2.

3.2. Membrane performance

Fig. 5 shows the DCMD fluxes of the prepared M1 (PES) and M2 (PEI) membranes along with those of the commercial membrane (FGLP 1425). Fig. 5a shows the DCMD flux vs. the average temperature of feed and permeate solutions (*Tm*) when distilled water was used as feed, while Fig. 5b shows the DCMD flux of the same membranes when using 0.5M NaCl aqueous solution as feed.

It is well documented that temperature is the operating variable that affects the MD flux the most due to the

Table 4
AFM analysis results of the membrane's prepared top surface

Surface characteristics	M1	M2
Mean pore size (d_p, nm)	21.50	22.38
Mean nodule size (nm)	33.30	29.58
Surface roughness (*R*, nm)	9.8	10.32
Geometric standard deviation (σ_p)	1.18	1.28

Table 5
Liquid entry pressure of water (LEP_w) and product of average pore size and effective porosity per unit effective pore length ($\varepsilon r/L_p$) of the laboratory prepared membranes

Membrane	LEP_w (bar)	$\varepsilon r/L_p$
M1	3.1	6.97×10^{-5}
M2	4.0	1.53×10^{-5}

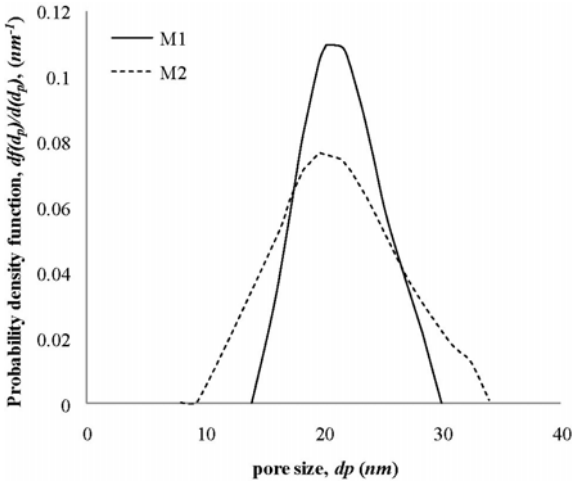

Fig. 4. Probability density function generated for the pore size measured from the AFM images.

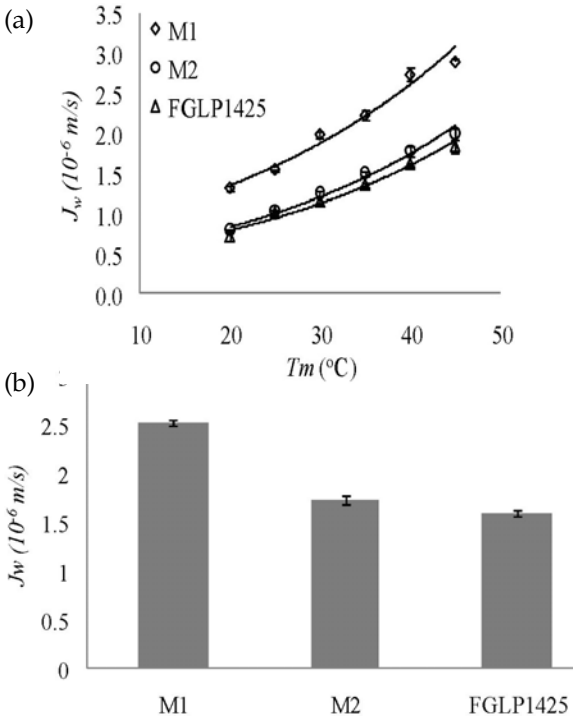

Fig. 5. DCMD flux result: (a) mean temperature effect on DCMD flux of distilled water feed solution; (b) water vapour flux of 0.5 M NaCl feed solution at *Tm* of 45°C.

exponential increase of vapour pressure with temperature according to the Antoine equation [1–7]. As shown in Fig. 5a, both the commercial membrane and SMM blended PES and PEI membranes exhibit an exponential increase of the DCMD flux with an increase in *Tm*.

Both Fig. 5a and 5b show that the order in the DCMD flux is M1 > M2 > FGLP 1425. In other words, the prepared SMM blended PES or PEI membranes showed higher permeate fluxes than the commercial membrane. In particular, the DCMD flux of the membranes M1 and M2 was found, on average within the tested temperatures, to be 65% and 8%, respectively, higher than that of the commercial membrane as shown in Fig.5a.

According to Table 5, the *LEPw* of those membranes under investigation followed the order of M2 > M1. This indicates that the order of the maximum pore size, according to the Laplace equation [14], should be M1 > M2 when the hydrophobicity of both membranes is equal. Moreover, Table 5 shows that the decreasing order of the ratio ($r\varepsilon/L_p$) is M1 > M2. The orders both in maximum pore size and $r\varepsilon/L_p$ agree with the order in the permeate flux. It can therefore be concluded that the membrane exhibiting a higher $r\varepsilon/L_p$ ratio will have higher DCMD flux. This is expected since an increase in the ratio means an increase in either the porosity and/or pore radius or a decrease in effective pore length.

According to the AFM data (see Table 4), the M1 membrane exhibited a smaller mean pore size compared to the M2 membrane. One can say that this contradicts the reported permeate flux result. But according to $r\varepsilon/L_p$ values, this flux enhancement is due to the increase of the effective porosity ratio, ε/L_p, which is greater for the M1 membrane.

As can be observed in Fig. 5b, smaller permeate fluxes were obtained in the presence of sodium chloride. The flux of M1, M2 and FGLP 1425 decreased by 13–15% compared to that obtained when distilled water was used as feed. Generally, it is expected to observe a flux decline in the presence of NaCl since the water vapor pressure decreases, which results in lower driving force for vapor transport. Moreover, a boundary layer develops next to the feed membrane surface where the NaCl concentration increases toward the membrane surface due to concentration polarization. The presence of the concentration boundary layer and the temperature boundary layer together reduces the driving force.

The solute separation factor defined earlier in Eq. (3) was higher than 99.9% (the permeate conductivity was always smaller than 25 μS/cm in all the tested membranes) for all the tested membranes. This indicates that the SMMs blended membranes M1 and M2 are considered promising for the MD process.

4. Conclusions

A better and instructive understanding of hydrophobic/hydrophilic membrane performance in MD has been obtained by finding the relationship between the membrane morphology and its performance in MD. This understanding can be summarized as follows:

- The higher product of average pore size and effective porosity per unit effective pore length ($r\varepsilon/L_p$) membranes produced higher fluxes. Membranes with higher liquid entry pressure of water (smaller maximum pore size) exhibited lower fluxes.
- Among the tested membrane preparation conditions it was found that the SMM/PES was a better membrane than the SMM/PEI membranes.
- Overall, both laboratory-made membranes exhibited higher fluxes than the commercial PTFE membrane, although they have considerably lower pore size and porosity. Moreover, the separation factor was higher than 99.9% for all tested membranes. Furthermore, it was proven that the SMMs are necessary to produce workable membranes in MD.

Acknowledgement

The authors of this work wish to gratefully acknowledge the Middle East Desalination Research Center (MEDRC) for a grant that partially supported this study.

References

[1] K.W. Lawson and D.R. Lloyd, Membrane distillation, J. Membr. Sci., 124 (1997) 1–25.
[2] J.I. Mengual and L. Peña, Membrane distillation, Curr. Topic Coll. Interf. Sci., 1 (1997) 17–29.
[3] A. Burgoyne and M.M. Vahdati, Direct contact membrane distillation, Sep. Sci. Technol., 35 (2000) 1257–1284.
[4] A.M. Alklaibi and N. Lior, Membrane-distillation desalination: Status and potential, Desalination, 171 (2004) 111–131.
[5] E. Curcio and E. Drioli, Membrane distillation and related operations — a review, Sep. Purif. Rev., 34 (2005) 35–86.
[6] M.S. El-Bourawi, Z. Ding, R. Ma and M. Khayet, A framework for better understanding membrane distillation separation process, J. Membr. Sci., 285 (2006) 4–29.
[7] L. Martínez, F.J. Florido-Díaz, A. Hernández and P. Prádanos, Characterization of three hydrophobic porous membranes used in membrane distillation: Modelling and evaluation of their water vapour permeabilities, J. Membr. Sci., 203 (2002) 15–27.
[8] M. Khayet, J.I. Mengual and T. Matsuura, Porous hydrophobic/hydrophilic composite membranes: Application in desalination using direct contact membrane distillation, J. Membr. Sci., 252 (2005) 101–113.
[9] M. Khayet, T. Matsuura, J.I. Mengual and M. Qtaishat, Design of novel direct contact membrane distillation membranes, Desalination, 192 (2006) 105–111.
[10] M. Khayet, T. Matsuura, M.R. Qtaishat and J.I. Mengual, Porous hydrophobic/hydrophilic composite membranes: Preparation and application in DCMD desalination at higher temperatures, Desalination, 199 (2006) 180–181.
[11] D.E. Suk, T. Matsuura, H.B. Park and Y.M. Lee, Synthesis of a new type of surface modifying macromolecules (nSMM) and characterization and testing of nSMM blended membranes for membrane distillation, J. Membr. Sci., 277 (2006) 177–185.
[12] M. Qtaishat, D. Rana, M. Khayet and T. Matsuura, Preparation and characterization of novel hydrophobic/hydrophilic polyetherimide composite membranes for desalination by direct contact membrane distillation, J. Membr. Sci., 327 (2009) 264–273.
[13] M. Khayet and T. Matsuura, Preparation and characterization of polyvinylidene fluoride membranes for membrane distillation, Ind. Eng. Chem. Res., 40 (2001) 5710–5718.
[14] P.C. Carman, Flow of Gases Through Porous Media, Butterworth, London, 1956.
[15] J. Barzin, C. Feng, K.C. Khulbe, T. Matsuura, S.S. Madaeni and H. Mirzadeh, Characterization of polyethersulfone hemodialysis membrane by ultrafiltration and atomic force microscopy, J. Membr. Sci., 237 (2004) 77–85.
[16] S. Singh, K.C. Khulbe, T. Matsuura and P. Ramamurthy, Membrane characterization by solute transport and atomic force microscopy, J. Membr. Sci., 142 (1998) 111–127.